

# Preparation of Nano-Porous Carbon-Silica Composites and Its Adsorption Capacity to Volatile Organic Compounds

## **Authors:**

Lipei Fu, Jiahui Zhu, Weiqiu Huang, Jie Fang, Xianhang Sun, Xinya Wang, Kaili Liao

*Date Submitted:* 2020-05-22

*Keywords:* dynamic adsorption, regenerating property, carbon-silica composites, Adsorption, volatile organic compounds (VOCs)

## **Abstract:**

Carbon-silica composites with nanoporous structures were synthesized for the adsorption of volatile organic compounds (VOCs), taking tetraethyl orthosilicate (TEOS) as the silicon source and activated carbon powder as the carbon source. The preparation conditions were as follows: the pH of the reaction system was 5.5, the hydrophobic modification time was 50 h, and the dosage of activated carbon was 2 wt%. Infrared spectrum analysis showed that the activated carbon was dispersed in the pores of aerogel to form the carbon-silica composites material. The static adsorption experiments, dynamic adsorption-desorption experiments, and regeneration experiments show that the prepared carbon-silica composites have microporous and mesoporous structures, the adsorption capacity for n-hexane is better than that of conventional hydrophobic silica gel, and the desorption performance is better than that of activated carbon. It still has a high retention rate of adsorption capacity after multiple adsorption-desorption cycles. The prepared carbon-silica composites material has good industrial application prospects in oil vapor recovery, providing a new alternative for solving organic waste gas pollution.

*Record Type:* Published Article

*Submitted To:* LAPSE (Living Archive for Process Systems Engineering)

*Citation (overall record, always the latest version):*

LAPSE:2020.0516

*Citation (this specific file, latest version):*

LAPSE:2020.0516-1

*Citation (this specific file, this version):*

LAPSE:2020.0516-1v1

*DOI of Published Version:* <https://doi.org/10.3390/pr8030372>

*License:* Creative Commons Attribution 4.0 International (CC BY 4.0)

Article

# Preparation of Nano-Porous Carbon-Silica Composites and Its Adsorption Capacity to Volatile Organic Compounds

Lipei Fu <sup>1,2</sup>, Jiahui Zhu <sup>1,2</sup>, Weiqiu Huang <sup>1,2,\*</sup>, Jie Fang <sup>1,2</sup>, Xianhang Sun <sup>1,2</sup>, Xinya Wang <sup>1,2</sup> and Kaili Liao <sup>1,2,\*</sup>

<sup>1</sup> School of Petroleum Engineering, Changzhou University, Changzhou 213164, China; fulipeiupc@163.com (L.F.); zhujiahui415@163.com (J.Z.); 17000189@smail.cczu.edu.cn (J.F.); sxh1987@cczu.edu.cn (X.S.); 18000647@smail.cczu.edu.cn (X.W.)

<sup>2</sup> Jiangsu Key Laboratory of Oil & Gas Storage and Transportation Technology, Changzhou University, Changzhou 213164, China

\* Correspondence: hwq213@cczu.edu.cn (W.H.); liaokaili@cczu.edu.cn (K.L.); Tel.: +86-135-0612-7318 (W.H.); +86-156-9520-7997 (K.L.)

Received: 21 February 2020; Accepted: 5 March 2020; Published: 23 March 2020



**Abstract:** Carbon-silica composites with nanoporous structures were synthesized for the adsorption of volatile organic compounds (VOCs), taking tetraethyl orthosilicate (TEOS) as the silicon source and activated carbon powder as the carbon source. The preparation conditions were as follows: the pH of the reaction system was 5.5, the hydrophobic modification time was 50 h, and the dosage of activated carbon was 2 wt%. Infrared spectrum analysis showed that the activated carbon was dispersed in the pores of aerogel to form the carbon-silica composites material. The static adsorption experiments, dynamic adsorption-desorption experiments, and regeneration experiments show that the prepared carbon-silica composites have microporous and mesoporous structures, the adsorption capacity for n-hexane is better than that of conventional hydrophobic silica gel, and the desorption performance is better than that of activated carbon. It still has a high retention rate of adsorption capacity after multiple adsorption-desorption cycles. The prepared carbon-silica composites material has good industrial application prospects in oil vapor recovery, providing a new alternative for solving organic waste gas pollution.

**Keywords:** volatile organic compounds (VOCs); adsorption; carbon-silica composites; regenerating property; dynamic adsorption

## 1. Introduction

The volatile organic compounds (VOCs) refer to organic compounds with the saturated vapor pressure of more than 70 Pa at room temperature, the boiling point of less than 260 °C at normal pressure, and they are usually present in the form of vapor in the air at normal temperature [1]. The emission sources of VOCs are divided into natural sources and man-made sources. On the global scale, VOCs emissions are mainly from natural sources. However, for the key regions and cities, emissions from man-made sources are much higher than those from natural sources, such as petrochemicals, oil and gas storage and transportation, pharmaceuticals, coatings, rubber, printing, and other processes [2]. A large amount of VOCs are generated in the above processes. The emission of VOCs in industrial processes not only causes serious air pollution but also causes huge economic losses [3]. VOCs not only have strong toxicity but also are key precursors of PM<sub>2.5</sub> and O<sub>3</sub>, which have important contributions to urban ash and photochemical pollution [4]. In recent years, governments all over the world have

proposed a series of VOCs pollution prevention policies and standards and imposed strict requirements to limit the emissions of industrial source VOCs.

Adsorption is the commonly used technology for VOCs treatment by virtue of its simple operations, as well as its user-friendliness character [5,6]. The use of effective physical adsorbents for organic gas adsorption and separation has been a hot research topic in the field of VOCs [7]. Activated carbon is the most widely used adsorbent because of its rich pore structure and large specific surface area [8,9]. In addition to the traditional coal-based activated carbon, biological activated carbons, such as rice husk and coconut shell activated carbon, have also been reported for VOCs treatment recently [10,11]. However, all kinds of activated carbons inevitably encounter the problem of low thermal conductivity, which are only 0.17–0.28 W/(m·K). It is well known that adsorption is an exothermic process, and if the heat released during the adsorption process cannot be conducted timely, it will affect the adsorption performance of the activated carbon. Especially in the industrial applications, the generated adsorption heat not only affects the adsorption efficiency but also may cause the adsorbent to overheat, which may cause the activated carbon combustion under aerobic conditions and bring a great safety hazard [12]. In addition, the lower thermal conductivity of activated carbon also directly affects the regeneration efficiency of activated carbon, which determines the economics of VOCs treatments [13]. In view of the poor thermal conductivity of the activated carbon, Kuwagaki et al. used expanded graphite to modify the walnut shell-based activated carbon; although the thermal conductivity was improved to a certain extent, it still could not meet the requirements for industrial application [14–16]. Poor regeneration performance means that the adsorption capacity will be greatly reduced after using for a period of time and eventually become solid waste, causing secondary pollution to the environment [17].

Silica gel is a porous silica hydrate with porous structure and can be used for VOCs adsorption after hydrophobic modifications [18]. It is found that, although hydrophobic silica gel has good regeneration properties, the adsorption capacity of VOCs is much lower than that of activated carbon, due to the larger diameter of the inner pores of the silica gel. Therefore, it can be used for the adsorption of low concentrations of VOCs treatments, while not suitable for that of high concentration VOCs treatments [19]. In addition, the aerogel is limited in application due to its poor mechanical strength. In view of the complementary relationship between the advantages and disadvantages of hydrophobic silica gel and activated carbon, it has been reported that the two kinds of adsorbent can be used in combination. The combination use means that the activated carbon and the hydrophobic silica gel were alternately filled in the adsorption bed. Usually, the upper layer is activated carbon, and the bottom layer is hydrophobic silica gel. Therefore, the advantages (such as the noncombustibility and the high regeneration rate of the hydrophobic silica gel and the large adsorption capacity of the activated carbon) can be comprehensively utilized, while the disadvantages (such as the limited adsorption capacity of the hydrophobic silica gel and the poor regeneration property of the activated carbon) can be overcome [20,21]. This adsorbent composite system based on the adsorption bed filling technology enables many chemical enterprises to meet the previous requirement that the total emission of non-methane hydrocarbon should be less than 0.5 g per liter of gasoline, which was issued earlier by the Ministry of Environment Protection of the People's Republic of China.

The Ministry of Environmental Protection raised the requirement that the total non-methane hydrocarbons emissions per liter of gasoline should not exceed 25 mg this year [22]. This standard imposed stricter requirements for VOCs emissions, and it is necessary to seek adsorbents with higher efficiency. At the same time, as the state implements strict control measures on solid waste, adsorbents, such as activated carbon, are required to have better regeneration performance to reduce the generation of solid waste and avoid secondary pollution to the environment. Mohammadi and Moghaddas proposed a carbon-silica composites adsorbent by using water glass as the silicon source and adding activated carbon (0.5 wt%) as the carbon source during the preparation of silica gel [23]. It had good performance in the adsorption evaluation of benzene and styrene. It also exhibited good adsorption performance after solvent extraction-thermal treatment. The regeneration rate could remain above 80% after 15 adsorption-desorption cycles. Lu et al. used commercially available mesoporous spherical silica

gel as the skeleton and sucrose as the carbon source to prepare a carbon-silica composites material. The evaluation experiments showed that the introduction of microporous carbon material into the channels of the silica gel can further improve the adsorption capacity, while maintaining the high thermal stability and mechanical strength of the silica gel. Encouragingly, the prepared carbon-silica composites had excellent desorption characteristics. The adsorbed toluene can be completely desorbed at 150 °C, which can be attributed to the formation of hierarchical pores of the carbon-silica composites [24]. This multi-scale pore size distribution not only facilitated the adsorption behaviors but also enabled gas molecules to be desorbed under two forces, namely self-desorption energy and the interaction between mesopores and micropores, effectively.

Motivated by the conclusion that carbon-silica composites have good adsorption property and excellent regeneration performance from the above discussions, we reported the preparation of carbon-silica composites by the traditional sol-gel method, taking tetraethyl orthosilicate (TEOS) as the silicon source and activated carbon powder as the carbon source [25]. Then, its application in oil vapor adsorption properties, such as the static adsorption property, dynamic adsorption property, and the regeneration performance, were studied. Due to the complex composition of oil vapor and the different volatility of each component, *n*-hexane, which accounts for a large proportion of oil vapor and has moderate volatility, was selected as the adsorbent for oil vapor adsorption capacity evaluation tests [26].

## 2. Materials and Methods

### 2.1. Materials

Tetraethyl orthosilicate (TEOS), analytically pure, was purchased from Sinopharm Chemical Reagent, Shanghai, China. Trimethylchlorosilane (TMCS), analytically pure, was purchased from Lingfeng Chemical, Shanghai, China. *N*-hexane with the purity of 95% was purchased from Qiangsheng Chemical, Shanghai, China. Powdered activated carbon was obtained from Xinsen Carbon Co., Ltd., Fujian, China. Ammonia water with the purity of 25%–28% was purchased from Lingfeng Chemical Co., Ltd., Shanghai, China. Gasoline was provided by Changzhou University.

### 2.2. Methods

#### 2.2.1. Preparation of Carbon-Silica Composites

The preparation scheme of the carbon-silica composites material is as follows: adding activated carbon powder during the preparation of the aerogel through sol-gel method, then giving hydrophobic properties to the composites materials by methylation reaction and thereby obtaining nano-porous carbon-silica composites adsorbent for VOCs adsorptions. Therefore, the preparation method is introduced in two parts, namely, the preparation method of the hydrophobic aerogel and the preparation method of the composites materials.

##### (1) Preparation method of the hydrophobic aerogel

① Preparing a diluent of TEOS (the molar ratio of TEOS, ethyl alcohol, and deionized water was TEOS:ETOH:H<sub>2</sub>O = 1:4:4); adjusting the pH value by using 0.1 mol/L hydrochloric acid to 1–2; and then the hydrogel was prepared. ② Placing and stirring the hydrogel in a water bath with the temperature of 60 °C for 2 h, adjusting the pH value by ammonia water (25 wt%) to 3–7 for gelling, and then putting it into the aging solution (TEOS:ETOH:NH<sub>4</sub>OH = 1:1:1 in volume ratio) for 24 h. ③ Placing the gel into the *n*-hexane solution with the temperature of 60 °C for 24 h. ④ Then, placing the gel into the hydrophobic modification liquid (TMCS:*n*-hexane = 1:4 in volume ratio) with the temperature of 60 °C for 12 h. ⑤ Washing the gel 3 times with the *n*-hexane solution, drying it at 150 °C for 2 h, and then the hydrophobic aerogel can be obtained.

## (2) Preparation of carbon-silica composites materials

Activated carbon powder (the dosage was 2% or 4% to the mass of the hydrogel) with the diameter of about 75  $\mu\text{m}$  was added into the hydrogel (between step ① and step ② in the process of hydrophobic aerogel preparation), keeping the other steps unchanged, and the carbon-silica composites adsorbent can be obtained. Wherein, if the mass percentage of the activated carbon (AC) added to the hydrogel (SG) was  $\alpha$ , the carbon-silica composites were recorded as SG/AC- $\alpha$ . Similarly, SG/AC-0 referred to the hydrophobic aerogel without activated carbon added.

### 2.2.2. Characterizing Methods

All the samples to be tested must be subjected to the drying treatment under a vacuum environment of 150  $^{\circ}\text{C}$  for 2 h. The  $\text{N}_2$  adsorption-desorption isotherm of the samples were measured by using an automatic physical/chemical analyzer (Autosorb-IQ2-2MP-V, Quantachrome, Boynton Beach, FL, USA) to obtain the parameters of the pore structure of the adsorbent, such as the specific surface area, pore volume, and pore size distribution [27]. The functional groups of the adsorbent samples were characterized by using the infrared spectrometer (Nicolet iS50, Thermo Fisher, Waltham, MA, USA).

### 2.2.3. Oil Vapor Adsorption Property Evaluation Tests

This method was used for the optimization of the hydrophobic aerogel preparation scheme, and the experimental device diagram is shown in Figure 1. The advantage of this method is its simplicity and quickness. The steps are as follows.

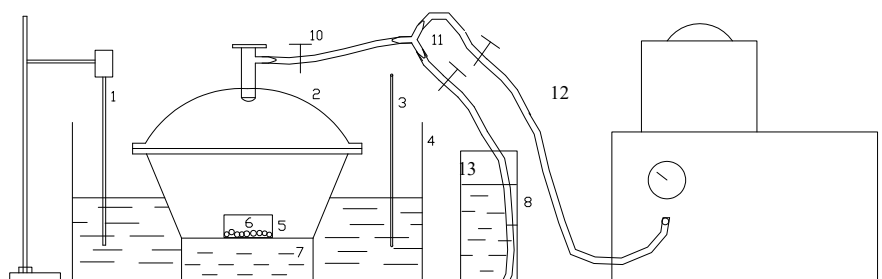


**Figure 1.** (Schematic diagram of the experimental equipment for oil vapor static adsorption: 1: stirrer; 2: vacuum retainer; 3: thermometer; 4: thermostatic water bath; 5: weighing bottle; 6: adsorbent; 7 and 8: adsorbates; 9: vacuum pump; 10, 12, and 13: valves; and 11: triple valves).

① Putting the pretreated adsorbent sample (its mass recorded as  $m_1$ ) into the weighing bottle and placing it (its mass recorded as  $m_2$ ) in the vacuum retainer (2). ② Closing the valve (12) after vacuuming the retainer (2). ③ Opening the valve (13), and the gasoline will be sucked into the retainer (2). ④ Closing all the valves when the mass of gasoline in the retainer does not change and waiting for the full evaporation of gasoline and making full contact between oil vapor and adsorbent. ⑤ Measuring the mass of the weighing bottle (its mass recorded as  $m_3$ ) after 10 h. The adsorption rate of hydrophobic aerogel to oil vapor can be calculated by the formula [3]:

$$X = \frac{(m_3 - m_2) - m_1}{m_1} \times 100\%$$

### 2.2.4. Static Adsorption Tests

The static adsorption-desorption performance of the adsorbent was determined by using a smart gravimetric adsorption analyzer (IGA-100B, Hiden Co., Warrington, UK). Its parameters were as follows: the accuracy of the balance and the thermometer were 0.1  $\mu\text{g}$  and 1  $^{\circ}\text{C}$ , respectively. The pretreated adsorbent sample was placed in the sample cell of the adsorption analyzer. *N*-hexane was

selected as the adsorbate instead of gasoline vapor. The adsorption rate can be calculated from the mass change of the adsorbate before and after adsorption.

### 2.2.5. Dynamic Adsorption Tests

The dynamic adsorption-desorption performance of the adsorbent was determined by using a self-made experimental setup, as shown in Figure 2. The test method was as follows: ① Placing an appropriate amount of the pretreated adsorbent sample into the cylindrical adsorption bed with the length of 40 cm and the diameter of 1 cm. ② The *n*-hexane vapor and N<sub>2</sub> were uniformly mixed in the gas mixing bottle, passed through the flow meter, and then entered the adsorption bed. During the process, the concentration of *n*-hexane and the flow rate of the mixture were controlled as 700 mg/L and 100 mL/min. ③ The concentrations of *n*-hexane at the inlet and outlet of the adsorption bed were measured by gas chromatograph (GC-2010 Plus, Shimadzu, Kyoto, Japan). The adsorption rate can be calculated according to the mass change of the adsorbent in the adsorption bed before and after adsorption.

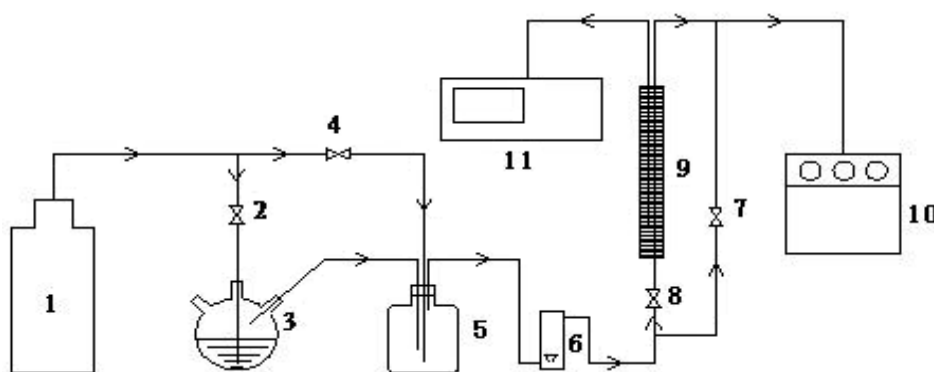


**Figure 2.** Figure 1 schematic diagram of the experimental equipment for oil vapor dynamic adsorption-desorption: 1: nitrogen cylinder; 2, 4, 7, and 8: valves; 3: *n*-hexane vapor generator; 5: gas mixing bottle; 6: rotor flow meter; 9: adsorption bed; and 10: gas chromatograph.

### 2.2.6. Regeneration Tests

The regeneration property is an important aspect to evaluate the performance of the adsorbent. The test method is as follows: In the dynamic adsorption-desorption experiment, the adsorption-desorption cycle was continuously performed, and the adsorption capacities of the same sample were recorded at each time. The regeneration performance of the carbon-silica composites was evaluated by comparing the change of the adsorption capacity.

## 3. Results

### 3.1. Silica Aerogel Preparation and Characterization

Silica aerogel is a kind of commonly used adsorbent, and the factors affecting its adsorption properties mainly include specific surface area, pore volume, and pore size. There are many factors that affect the above structural parameters in the preparation process, such as the pH value of the reaction system, the type of the hydrophobic modifier, the modification time, the aging temperature, and the reactant ratio. According to previous studies, the pH value of the system in the gelation process and the hydrophobic modification time have obvious effects on the pore structure and the adsorption performance of hydrophobic aerogel [3]. Therefore, the effects of the mentioned factors were studied, and the optimal preparation conditions were optimized accordingly.

### 3.1.1. pH Value

In the gelation process, the pH value of the system was controlled as 3.8, 4.8, 5.5, and 6.5, respectively, by changing the amount of ammonia water so as to study the pH value on the adsorption performance and pore structure of hydrophobic aerogel. The hydrophobic modification time was 50 h in all the mentioned tests. The experimental results are shown in Figures 3 and 4. The adsorption performances of the aerogels prepared under different pH values were evaluated by oil vapor adsorption property evaluation tests. The results, as well as the pore structure parameters of each aerogel, are shown in Table 1.

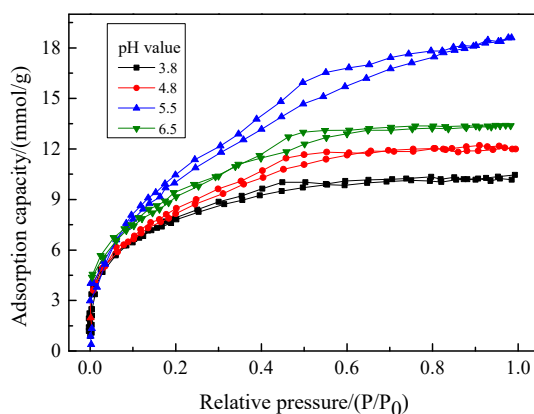


Figure 3.  $N_2$  adsorption-desorption isotherms of the aerogels prepared at different pH values.

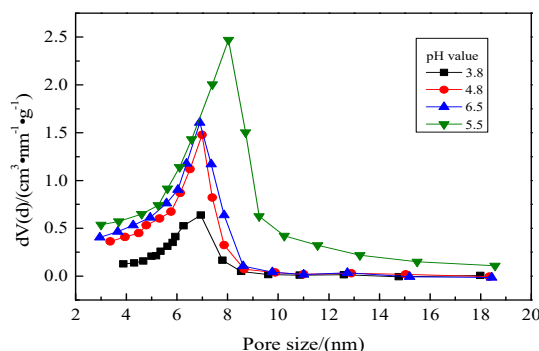


Figure 4. Pore size distributions of the aerogels prepared at different pH values.

Table 1. Pore structure characteristics and oil vapor adsorption rates of aerogels prepared at different pH values.

| pH Value | Specific Surface Area ( $m^2/g$ ) | Pore Volume ( $cm^3/g$ ) | Average Pore Size (nm) | Oil Vapor Adsorption Rate (%) |
|----------|-----------------------------------|--------------------------|------------------------|-------------------------------|
| 3.8      | 614                               | 0.36                     | 2.32                   | 21.28                         |
| 4.8      | 692                               | 0.42                     | 2.40                   | 22.37                         |
| 5.5      | 713                               | 0.64                     | 2.95                   | 23.67                         |
| 6.5      | 707                               | 0.39                     | 2.51                   | 22.83                         |

It can be seen from Figure 3 that the  $N_2$  adsorption-desorption isotherms of aerogels prepared under different pH value conditions have obvious hysteresis loops, belonging to type IV isotherm, indicating that the hydrophobic silica gel prepared under different pH values were mainly mesoporous. From Table 1, it can be found that as the pH value increases from 3.8 to 6.5, the specific surface area of the hydrophobic silica gel increases from  $614 m^2/g$  to  $713 m^2/g$  and then decreases to  $707 m^2/g$ , while the total pore volume increases from  $0.36 cm^3/g$  to  $0.64 cm^3/g$  and then decreases to  $0.39 cm^3/g$ . It indicates that the aerogel has the highest specific surface area and total pore volume when the pH value

is 5.5. In addition, when the pH value is 5.5, the pore size distribution of the prepared hydrophobic silica gel is about 8 nm, while that is 7 nm when the pH value is 3.8, 4.8, and 6.5, which can be seen in Figure 4. Comparing the parameters in Table 1, it can be seen that the aerogel prepared when the pH value was 5.5 has better pore structure and adsorption performance.

### 3.1.2. Treating Time

The treating time of hydrophobic modification directly influences the hydrophobic properties of the aerogel, which further affects its adsorption capacity for VOCs. Therefore, the effects of treating time on the pore structure and adsorption performance of the hydrophobic aerogel were investigated. The treating time was set to 2 h, 25 h, 50 h, and 62 h, respectively, and the pH value of the reaction system was 5.5. The results are shown in Figures 5 and 6. The oil vapor adsorption rates of the corresponding aerogels are shown in Table 2.

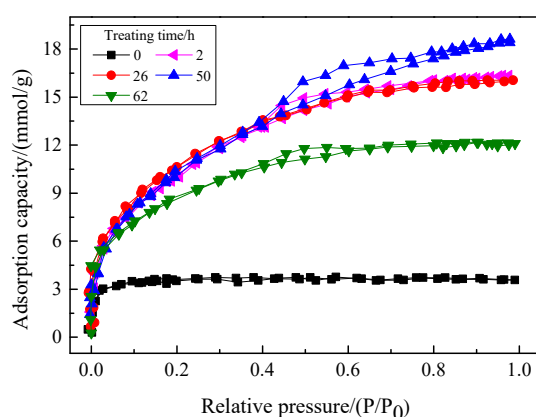


**Figure 5.**  $N_2$  adsorption-desorption isotherms of the aerogels prepared at different treating times.

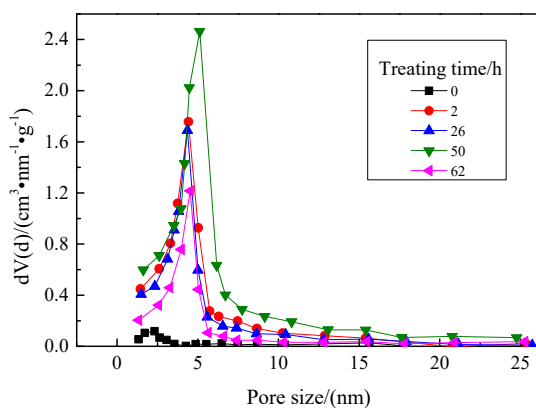


**Figure 6.** Pore size distributions of the aerogels prepared at different treating times.

**Table 2.** Pore structure characteristics and oil vapor adsorption rates of aerogels prepared at different treating times.

| Treating Time (h) | Specific Surface Area ( $m^2/g$ ) | Pore Volume ( $cm^3/g$ ) | Average Pore Size (nm) | Oil Vapor Adsorption Rate (%) |
|-------------------|-----------------------------------|--------------------------|------------------------|-------------------------------|
| 0                 | 251                               | 0.13                     | 2.02                   | 12.19                         |
| 2                 | 649                               | 0.56                     | 2.58                   | 22.33                         |
| 26                | 675                               | 0.57                     | 2.54                   | 22.47                         |
| 50                | 724                               | 0.70                     | 3.80                   | 26.83                         |
| 62                | 715                               | 0.42                     | 2.43                   | 23.41                         |



It can be seen from Figure 5 that the  $N_2$  adsorption-desorption isotherms of aerogels prepared under different treating times of hydrophobic modifications have obvious hysteresis loops, belonging to type IV isotherm, indicating that the hydrophobic aerogel prepared under different pH values were mainly mesoporous. The aerogel that has not been hydrophobically modified has no hysteresis loops. The reason lies in the subsequent drying shrinkage stage. Additionally, it can be known that, under high pressure ( $P/P_0 \geq 0.5$ ), the  $N_2$  adsorption-desorption isotherm was at the top when the treating time was 50 h, while the isotherm was at the bottom when the treating time was 0 h. In addition, it can be seen from Table 2 that, as the treating time of hydrophobic modification increases from 0 h to 62 h, the specific surface area of the hydrophobic aerogel increases from  $251 \text{ m}^2/\text{g}$  to  $724 \text{ m}^2/\text{g}$  and then decreases to  $715 \text{ m}^2/\text{g}$ , while the total pore volume increases from  $0.13 \text{ cm}^3/\text{g}$  to  $0.70 \text{ cm}^3/\text{g}$  and then decreases to  $0.42 \text{ cm}^3/\text{g}$ . It indicates that the aerogel has the highest specific surface area and total pore volume when the treating time is 50 h.

From the pore size distribution diagram of Figure 6, it can be known that, when the treating time is 50 h, the pore size of the aerogel is about 6 nm, while that was 5 nm when the treating time is 2 h, 25 h, and 62 h. Comparing the parameters in Table 2, it can be seen that the aerogel prepared hydrophobically by treating for 50 h has better pore structure and adsorption performance.

In summary, when the hydrophobic aerogel is prepared by the gel-sol method, the pH value of the reaction system should be 5.5, and the hydrophobic modification time should be 50 h.

### 3.1.3. Physicochemical Characteristics

The physical and chemical characterizations of hydrophobic aerogel prepared under the optimal conditions were carried out. The  $N_2$  adsorption-desorption isotherms at 77 K are shown in Figure 7. The pore size distribution obtained according to the BJH calculation method is shown in Figure 8 [28]. The Fourier transform infra-red (abbreviated as FTIR) spectrums of the hydrophobically modified aerogel and the untreated aerogel are shown in Figure 9.

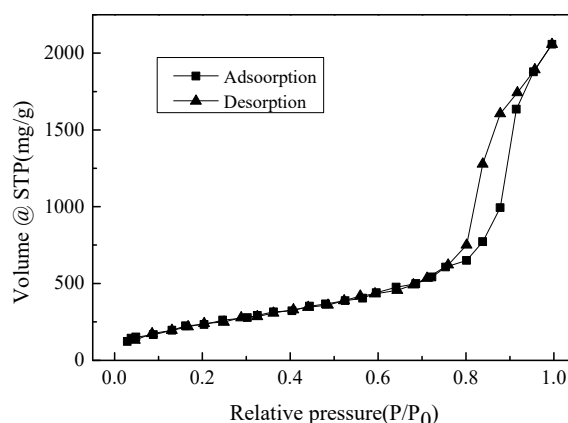


**Figure 7.**  $N_2$  adsorption-desorption isotherms of the silica aerogels prepared under the optimum condition.

It can be seen from Figure 7 that, when the relative pressure is lower than 0.6, the adsorption amount of the hydrophobic aerogel increases slowly as the relative pressure increases, while, when the relative pressure is 0.6 to 0.9, the adsorption-desorption isotherms have obvious hysteresis loops. According to the definition of the International Union of Pure and Applied Chemistry (IUPAC 2015), the mentioned isotherm belongs to type IV(a), and the hysteresis loop belongs to type  $H_2$ . Based on the relationship between hysteresis loop and pore shape, it can be inferred that the hydrophobic aerogel is filled with cylindrical pores. It can be calculated that the specific surface area of the hydrophobic aerogel was about  $724 \text{ m}^2 \cdot \text{g}^{-1}$ , and the total pore volume was about  $0.70 \text{ m}^3 \cdot \text{g}^{-1}$  (when the relative pressure  $P/P_0$  was 0.995).

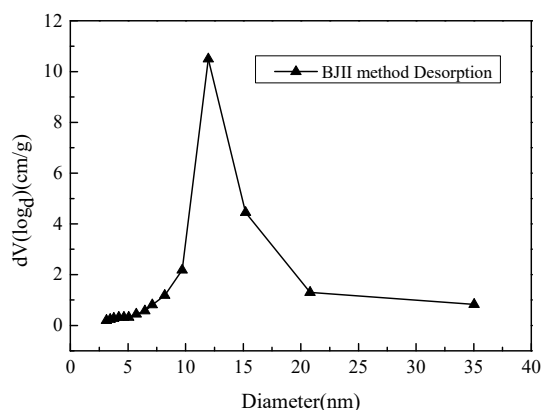


**Figure 8.** Pore size distributions of hydrophobic silica aerogel prepared under the optimum condition.

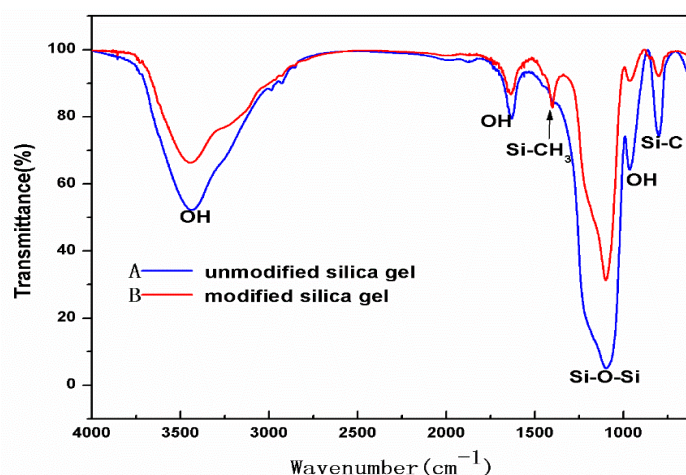


**Figure 9.** Fourier transform infra-red (FTIR) spectra of samples of unmodified silica aerogel and hydrophobic silica aerogel.

As can be seen from Figure 8, the hydrophobic aerogel prepared is a typical mesoporous material. The diameter of the pores is mainly distributed in the range of 10–20 nm.

In Figure 9, curve B is the spectrogram of the aerogel modified by TMCS and curve A is that of the untreated aerogel. It can be found that the characteristic peaks of OH groups at  $3500\text{ cm}^{-1}$  and  $1630\text{ cm}^{-1}$  and asymmetric and symmetric modes of  $\text{SiO}_2$  at  $1100\text{ cm}^{-1}$  and  $800\text{ cm}^{-1}$  are all exhibited in curve A and curve B [29]. The difference is that the modified silica gel has a distinct characteristic peak around  $1400\text{ cm}^{-1}$ , which is the characteristic peak of the CH group, indicating that the  $-\text{CH}_3$  in the silane has been successfully attached to the silica gel skeleton, thus giving the aerogel silica gel hydrophobic properties [30].

### 3.2. Carbon-Silica Composites Preparation

#### 3.2.1. Effect of the Carbon Content on Pore Structure

The carbon content affects the pore structure of the carbon-silica composites, which further affects its adsorption performance. For this reason, nitrogen adsorption-desorption measurements at 77 k were carried out on samples with different carbon contents, and the pore size distribution was obtained by BJH model calculation, as shown in Figures 10 and 11 and Table 3. The hydrophobic aerogel (SG/AC-0, meaning the carbon content was 0%) and the pure activated carbon were conducted as control tests.

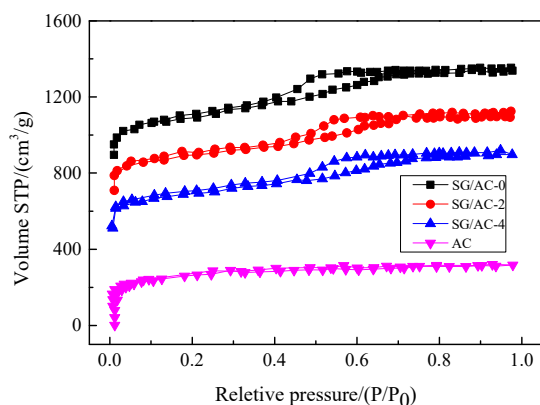


**Figure 10.** N<sub>2</sub> adsorption-desorption isotherms of the carbon-silica composites, hydrophobic silica aerogel, and active carbon.

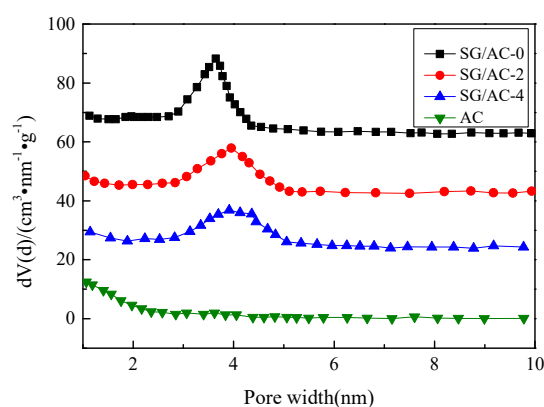


**Figure 11.** Pore size distributions of carbon-silica composites, hydrophobic silica aerogel, and active carbon.

**Table 3.** Pore structure parameters of carbon-silica composites, hydrophobic silica aerogel, and active carbon.

| Sample Name | Specific Surface Area (m <sup>2</sup> /g) | Average Pore Size (nm) | Volume of Micropore (cm <sup>3</sup> /g) | Specific Surface Area of Microporous (m <sup>2</sup> /g) | Volume of Total Pore (cm <sup>3</sup> /g) |
|-------------|---|------------------------|--|--|---|
| SG/AC-0     | 724                                       | 3.8                    | -  | -  | 0.70                                      |
| SG/AC-2     | 725                                       | 3.5                    | 0.05                                     | 101  | 0.67                                      |
| SG/AC-4     | 718                                       | 3.4                    | 0.06                                     | 109  | 0.65                                      |
| AC          | 925                                       | 2.1                    | 0.32                                     | 710  | 0.51                                      |

It can be seen from Figure 10 that hydrophobic aerogel (SG/AC-0) and carbon-silica composites (SG/AC-2 and SG/AC-4) have obvious H<sub>2</sub> hysteresis loops and the isotherms belong to type IV, while the isotherm of activated carbon belongs to type I. Combined with the pore size distribution (as shown in Figure 11) and the pore parameters (as shown in Table 3), it is known that the activated carbon belongs to a typical microporous structure. The pore structure of the hydrophobic aerogel and carbon-silica composites are mainly mesoporous, supplemented by microporous. With the increase of the content of activated carbon, the volume of micropores increases, and the volume of total pores decreases. The pore structure distribution of the SG/AC-2 is optimal.

In summary, SG/AC-2 has a better microporous structure than SG/AC-0 and has a larger specific surface area and total pore volume than SG/AC-4, which is an ideal adsorbent material. Therefore, SG/AC-2 was selected as the research object, and the static adsorption tests, dynamic adsorption tests, and regeneration performance evaluation tests of *n*-hexane were carried out.

### 3.2.2. FTIR Analysis

Infrared spectroscopy analysis was carried out for the carbon-silica composites (SG/AC-2) and the hydrophobic aerogel (SG/AC-0) to study the functional groups. The results are shown in Figure 12. It can be seen from Figure 12 that SG/AC-2 retained the main peaks of SG/AC-0, such as OH groups at  $3500\text{ cm}^{-1}$  and  $1630\text{ cm}^{-1}$ , asymmetric and symmetric modes of  $\text{SiO}_2$  at  $1100\text{ cm}^{-1}$  and  $800\text{ cm}^{-1}$ , and CH groups around  $1400\text{ cm}^{-1}$  [26,29]. In addition, SG/AC-2 also showed a new adsorption peak at  $750\text{ cm}^{-1}$ , which belongs to the Si-C group, indicating that the powdered activated carbon has been dispersed in the nanostructure pores in aerogel and formed carbon-silica composites [23].

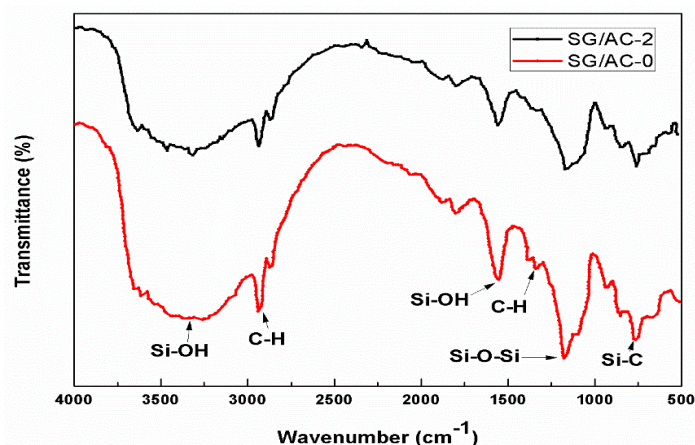


**Figure 12.** FTIR spectra of samples of carbon-silica composites, hydrophobic silica aerogel.

### 3.3. Static Adsorption Properties

The static adsorption-desorption performance of the carbon-silica composites material was tested by the smart gravimetric adsorption analyzer. The hydrophobic aerogel SG/AC-0 and the activated carbon AC were also determined as the control tests. The results are shown in Figure 13.

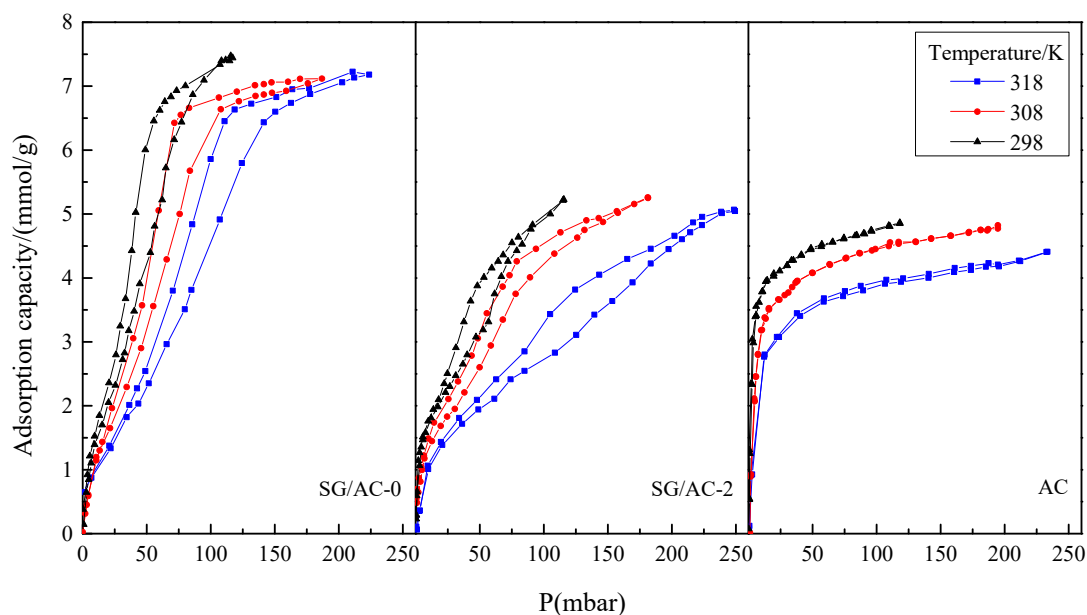


**Figure 13.** Static adsorption-desorption isotherms of *n*-hexane on SG/AC-0, SG/AC-2, and AC at different temperatures.

It can be found that the three candidates are similar in the  $\text{N}_2$  adsorption-desorption isotherms. At three temperatures, the adsorption growth rate of *n*-hexane at low pressure is significantly different,

and the order from large to small is  $AC > SG/AC-2 > SG/AC-0$ . The reason for this phenomenon is that the structures of the micropores of the three materials are different. The larger the specific surface area and the pore volumes of the micropores, the greater the adsorption force between the adsorbent and the adsorbate and the higher the adsorption rate was. Compared with AC, SG/AC-0 and SG/AC-2 have obvious nonoverlapping isotherms on *n*-hexane adsorption-desorption, which is mainly because both of SG/AC-0 and SG/AC-2 have rich mesoporous structures. At the same time, the nanoporous pores and throats give them the dual adsorption characteristics of micropores and mesopores.

The equilibrium adsorption capacities of the three adsorbents of SG/AC-0, SG/AC-2, and AC for *n*-hexane are shown in Figure 14. It can be found that, as the temperature increases, the equilibrium adsorption capacities of the three materials to *n*-hexane decreases, indicating that the temperature will affect the adsorption capacity, which is due to the thermal motion of molecules of the *n*-hexane vapor caused by temperature. In addition, at the three temperatures, the order of equilibrium adsorption capacity is  $SG/AC-0 > SG/AC-2 > AC$ . Combined with the pore volumes of the three materials in Table 3, the adsorption capacity of the three materials mainly depends on the pore volumes [26]. By comparing the influence of the above factors of temperature and pore structure on its adsorption performance, it is known that the pore structure of the material is the main factor.

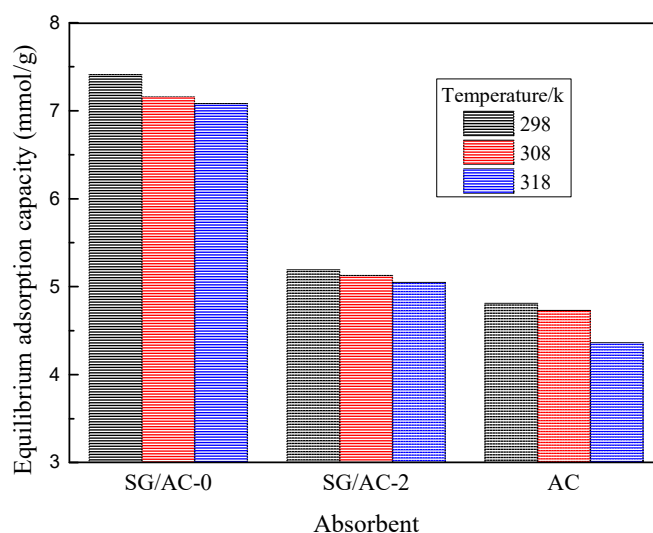


**Figure 14.** Equilibrium adsorption capacities of *n*-hexane on carbon-silica composites, hydrophobic silica aerogel, and active carbon at different temperatures.

Therefore, the hydrophobic aerogel with larger pore volume has the best static adsorption capacity, followed by the carbon-silica composites with microporous and mesoporous structures, and the activated carbon with microporous structure was the worst.

### 3.4. Dynamic Adsorption Properties

In order to further investigate the adsorption performance of carbon-silica composites on *n*-hexane under industrial conditions, a dynamic adsorption-desorption experiment was carried out. In the dynamic experiment, the concentration of *n*-hexane at the outlet was taken as the index to evaluate the adsorption speed and penetration performance. The adsorption penetration curve and desorption curve are shown in Figure 15. At the same time, the mass of adsorbents before and after *n*-hexane adsorption were measured to evaluate its adsorption capacity from another perspective. The results are shown in Table 4.

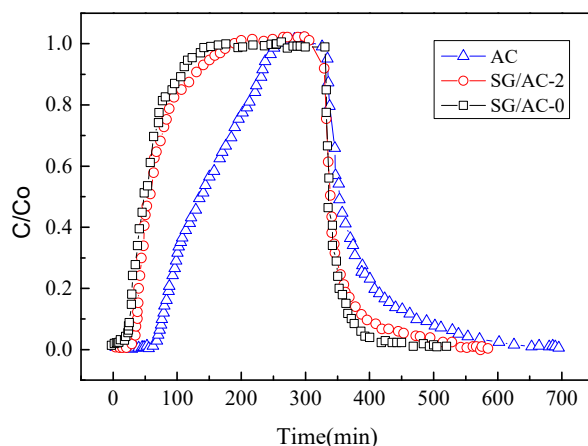


**Figure 15.** Breakthrough curves and desorption curves of *n*-hexane adsorption (0–300 min)/desorption (300–700 min) on carbon-silica composites, hydrophobic silica aerogel, and active carbon at ambient temperatures and pressures.

**Table 4.** Dynamic adsorption capacities of carbon-silica composites, hydrophobic silica aerogel, and active carbon.

| Adsorbent | Dynamic Adsorption Capacities (mmol/g) |
|-----------|--|
| SG/AC-0   | 0.89                                   |
| SG/AC-2   | 1.59                                   |
| AC        | 3.99                                   |

As can be seen from Figure 15, during the adsorption stage (0–300 min), activated carbon has the longest penetration time, followed by carbon-silica composites, and hydrophobic aerogel has the shortest penetration time, indicating that activated carbon has the strongest dynamic adsorption performance. The reason for this phenomenon is that the pore structure of the three materials is different. The pore diameter of mesoporous is large, so that the adsorption speed in dynamic adsorption is relatively fast. However, the pore diameter of micropores is small, and it is difficult for the gas molecules to enter, so the penetration time is long. The longer the penetration time is, the more gas can be adsorbed. The adsorption performance evaluation based on the mass method in Table 4 also illustrates this property. Therefore, the results of dynamic adsorption experiments showed that, compared with aerogel SG/AV-0, the carbon-silica composites SG/AC-2 has higher adsorption capacity, while compared with activated carbon AC, the carbon-silica composites SG/AC-2 has lower mass transfer resistance.

In the desorption stage (300–700 min), the desorption time of activated carbon AC was the longest (400 min), and the desorption time difference between carbon-silica composites and hydrophobic aerogel was relatively small (they were 300 min and 230 min, respectively). The reason is that the ratio of micropores of the three materials is different, as shown in Table 3. Due to the capillary condensation phenomenon in the micropores, *n*-hexane is difficult to be desorbed from the micropores, so the desorption time required for adsorbents with more micropores is relatively long.

Therefore, due to the high adsorption capacity of carbon silica composites to *n*-hexane (compared with aerogel) and the relatively low mass transfer resistance (compared with activated carbon), the relatively balanced adsorption-desorption performance makes the carbon-silica composites more suitable for industrial applications in *n*-hexane adsorption and recovery.

### 3.5. Regenerating Properties

In the industrial application of adsorbents for oil vapor recovery, the regeneration performance of the adsorbent is an important indicator to evaluate its industrial applicability. The adsorbent

with excellent performance needs to maintain good adsorption performance after multiple rounds of adsorption-desorption cycles. Therefore, the regeneration properties of the prepared aerogel and carbon-silica composites were evaluated, and the experimental results are shown in Figures 16 and 17, respectively.

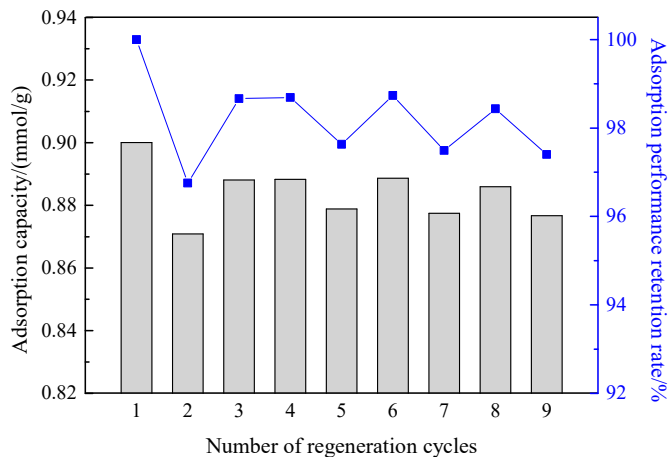


**Figure 16.** Dynamic adsorption capacity and adsorption retention rates of hydrophobic silica aerogel after different regeneration cycles.

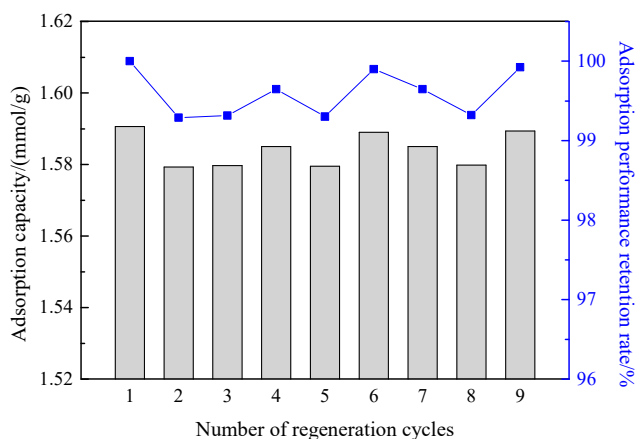


**Figure 17.** Dynamic adsorption capacity and adsorption retention rates of carbon-silica composites after different regeneration cycles.

The left axes of Figures 16 and 17 are the dynamic adsorption capacity, and the right axes are the adsorbent adsorption retention rates. It can be seen from the figures that, after nine times of dynamic adsorption-desorption processes, the adsorption capacity of aerogel and carbon-silica composites were still 0.88 mmol/g and 1.59 mmol/g, and the retention rates of the adsorption capacity were up to 97% and 99.5%, respectively. This shows that the prepared carbon-silica composites material has good regeneration performance in the dynamic process, can be recycled, and has industrial application promotion value.

#### 4. Conclusions

Carbon-silica composites were prepared by sol-gel method based on the preparation of hydrophobic aerogel. The preparation condition was that the pH of the reaction system should be 5.5, the hydrophobic modification time should be 50 h, and the dosage of activated carbon should be 2 wt%. Its specific surface area was 725 m<sup>2</sup>/g, average pore size was 3.5 nm, and total pore volume was 0.67 cm<sup>3</sup>/g. The equilibrium adsorption capacities of hydrophobic aerogel, carbon-silica composites, and activated carbon for *n*-hexane were 7.16 mmol/g, 5.13 mmol/g, and 4.73 mmol/g, respectively, indicating

that the adsorption performance of carbon-silica composites with microporous and mesoporous structures to *n*-hexane is better than that of activated carbon with microporous structures. In dynamic adsorption experiments, their equilibrium adsorption capacities were 0.89 mmol/g, 1.59 mmol/g, and 3.99 mmol/g, and the desorption times were 230 min, 300 min, and 400 min, indicating that carbon-silica composites have a relatively high adsorption capacity for *n*-hexane and a relatively small mass transfer resistance. Its retention rate of adsorption capacity was up to 99.5% after nine times of the dynamic adsorption-desorption processes, showing that carbon-silica composites has good regeneration performance in the dynamic process and can be recycled. The above results show that the carbon-silica composites with balanced adsorption-desorption performance has good industrial application prospects in oil vapor recovery and provides a new alternative for solving VOCs pollutions.

**Author Contributions:** Conceptualization, W.H. and L.F.; methodology, J.F. and J.Z.; validation, X.W., X.S., and J.Z.; formal analysis, K.L.; investigation, L.F.; resources, X.S.; data curation, J.Z.; writing—original draft preparation, L.F.; writing—review and editing, J.Z. and K.L.; visualization, X.S.; and supervision, W.H. All authors have read and agreed to the published version of the manuscript.

**Acknowledgments:** The research was funded by the National Natural Science Foundation of China (No. 51804045 and No. 51574044), the Key Research and Development Program of Jiangsu Province (Industry Foresight and Common Key Technology) (No. BE2018065), the Sci & Tech Program of Changzhou (No. CJ20180053), and the Postgraduate Research & Practice Innovation Program of Jiangsu Province (NO. KYCX19\_1786 and NO. SJCX19\_0668) are gratefully acknowledged.

**Conflicts of Interest:** The authors declare no conflicts of interest.

## References

1. Yang, C.; Miao, G.; Pi, Y.; Xia, Q.; Wu, J.; Li, Z.; Xiao, J. Abatement of various types of VOCs by adsorption/catalytic oxidation: A review. *Chem. Eng. J.* **2019**, *370*, 1128–1153. [[CrossRef](#)]
2. Lhuissier, M.; Couvert, A.; Amrane, A.; Kane, A.; Audic, J. Characterization and selection of waste oils for the absorption and biodegradation of VOC of different hydrophobicities. *Chem. Eng. Res. Des.* **2018**, *138*, 482–489. [[CrossRef](#)]
3. Huang, W.; Xu, J.; Tang, B.; Wang, H.; Tan, X.; Lv, A. Adsorption performance of hydrophobically modified silica gel for the vapors of *n*-hexane and water. *Adsorpt. Sci. Technol.* **2018**, *36*, 888–903. [[CrossRef](#)]
4. Zhang, X.; Gao, B.; Creamer, A.E.; Cao, C.; Li, Y. Adsorption of VOCs onto engineered carbon materials: A review. *J. Hazard. Mater.* **2017**, *338*, 102–123. [[CrossRef](#)]
5. Zhang, G.; Feizbakhshan, M.; Zheng, S.; Hashisho, Z.; Sun, Z.; Liu, Y. Effects of properties of minerals adsorbents for the adsorption and desorption of volatile organic compounds (VOC). *Appl. Clay Sci.* **2019**, *173*, 88–96. [[CrossRef](#)]
6. Long, Y.; Wu, S.; Xiao, Y.; Cui, P.; Zhou, H. VOCs reduction and inhibition mechanisms of using active carbon filler in bituminous materials. *J. Clean. Prod.* **2018**, *181*, 784–793. [[CrossRef](#)]
7. Giraudet, S.; Pré, P.; Tezel, H.; Le Cloirec, P. Estimation of adsorption energies using the physical characteristics of activated carbons and the molecular properties of volatile organic compounds. *Carbon* **2006**, *44*, 2413–2421. [[CrossRef](#)]
8. Liu, F.; Dai, Y.; Zhang, S.; Li, J.; Zhao, C.; Wang, Y.; Liu, C.; Sun, J. Modification and application of mesoporous carbon adsorbent for removal of endocrine disruptor bisphenol A in aqueous solutions. *J. Mater. Sci.* **2018**, *53*, 2337–2350. [[CrossRef](#)]
9. Zhao, Z.; Wang, S.; Yang, Y.; Li, X.; Li, J.; Li, Z. Competitive adsorption and selectivity of benzene and water vapor on the microporous metal organic frameworks (HKUST-1). *Chem. Eng. J.* **2015**, *259*, 79–89. [[CrossRef](#)]
10. Xu, J.; Huang, W.; Wang, Y.; Huang, F.; Zhao, S.; Hao, Q. Preparation of activated carbon from the desilication residue of rice husk and adsorption of oil vapor. *New Chem. Mater.* **2017**, *45*, 212–217.
11. Tan, X.; Huang, W.; Wang, Y.; Huang, F.; Zhu, Y.; Xu, J.; Qin, X. Hydrophobic modification of silica-gel based on rice husk and its adsorption property for oil vapor. *New Chem. Mater.* **2017**, *45*, 236–238.
12. Su, Z.; Pan, N.; Zhao, W.; Mo, J.; Xi, H. Preparation and properties of activated carbons with high thermal conductivity. *Chem. Eng. N. Y.* **2012**, *40*, 14–18.
13. Gu, X.; Huang, Y. Preparation of activated carbons with high thermal conductivity and its microwave regeneration performance research. *Henan Chem. Ind.* **2018**, *35*, 24–26.



14. Kuwagaki, H.; Meguro, T.; Tatami, J.; Tamura, K. An improvement of thermal conduction of activated carbon by adding graphite. *J. Mater. Sci.* **2003**, *38*, 3279–3284. [[CrossRef](#)]
15. Menard, D.P.X.; Mazet, N. Activated carbon monolith of high thermal conductivity for adsorption processes improvement: Part A: Adsorption step. *Chem. Eng. Process.* **2005**, *44*, 1029–1038. [[CrossRef](#)]
16. Pan, N.; Su, Z.; Mo, J.; Xi, H.; Xia, Q.; Li, Z. Preparation of novel composite activated carbon with high applicability to microwave and its regeneration under microwave radiation. *Chin. J. Chem. Eng.* **2011**, *62*, 111–118.
17. Zhang, Y.; Jiang, C.; Zhang, H. Research of Absorbent Materials for Volatile Organic Compounds. *Safe Health Environ.* **2016**, *16*, 1–6.
18. Walcarius, A.; Mercier, L. Mesoporous organosilica adsorbents: Nanoengineered materials for removal of organic and inorganic pollutants. *J. Mater. Chem.* **2010**, *20*, 4478–4511. [[CrossRef](#)]
19. Wang, Y.; Huang, W.; Lv, Y.; Wang, W.; Wang, Y. Investigation of modified hydrophobic silica gel for gasoline vapor adsorption and desorption. *Chin. J. Environ. Eng.* **2015**, *9*, 855–891.
20. Huang, W.; Bai, J.; Shen, Y. Composites adsorbent of activated and hydrophobic silica gel for gasoline vapor recovery. *Chem. Eng. N. Y.* **2011**, *39*, 38–41.
21. Nagata, T.; Tajima, H.; Yamasaki, A.; Kiyono, F.; Abe, Y. An analysis of gas separation processes of HFC-134a from gaseous mixtures with nitrogen—Comparison of two types of gas separation methods, liquefaction and hydrate-based methods, in terms of the equilibrium recovery ratio. *Sep. Purif. Technol.* **2009**, *64*, 351–356. [[CrossRef](#)]
22. Wang, H.; Li, Z.; Huang, W.; Shen, F.; Xu, C.; Zhong, J.; Chen, R. Controllable synthesis of hollow silica spheres and their adsorption to VOCs. *Mod. Chem. Ind.* **2019**, *39*, 99–104.
23. Mohammadi, A.; Moghaddas, J. Synthesis, adsorption and regeneration of nanoporous silica aerogel and silica aerogel-activated carbon composites. *Chem. Eng. Res. Des.* **2015**, *94*, 475–484. [[CrossRef](#)]
24. Lu, X.; He, J.; Xie, J.; Zhou, Y.; Liu, S.; Zhu, Q.; Lu, H. Preparation of hydrophobic hierarchical pore carbon–silica composites and its adsorption performance toward volatile organic compounds. *J. Environ. Sci. China* **2020**, *87*, 39–48. [[CrossRef](#)]
25. Zhang, W.; Li, Y.; Wang, Q.; Ren, M.; Zhu, G. Studies on the surface modification and thermal stability of silica aerogels. *J. Jilin Norm. Univ.* **2009**, *30*, 67–69.
26. Li, X.; Huang, W.; Liu, X.; Bian, H. Graphene oxide assisted ZIF-90 composites with enhanced n-hexane vapor adsorption capacity, efficiency and rate. *J. Solid State Chem.* **2019**, *278*, 120–890. [[CrossRef](#)]
27. Zhang, W.; Huang, B.; Yu, X.; Zhang, J. Interpretation of BJH Method for Calculating Aperture Distribution Process. *Univ. Chem.* **2020**, *35*, 98–106.
28. Țălu, Ș. *Micro and Nanoscale Characterization of Three Dimensional Surfaces: Basics and Applications*; Napoca Star Publishing House: Cluj-Napoca, Romania, 2015; ISBN 978-60-6690-349-3.
29. Rao, A.P.; Rao, A.V.; Pajonk, G.M. Hydrophobic and physical properties of the ambient pressure dried silica aerogels with sodium silicate precursor using various surface modification agents. *Appl. Surf. Sci.* **2007**, *253*, 6032–6040. [[CrossRef](#)]
30. Shi, F.; Wang, L.; Liu, J. Synthesis and characterization of silica aerogels by a novel fast ambient pressure drying process. *Mater. Lett.* **2006**, *60*, 3718–3722. [[CrossRef](#)]

